

vertebrates except in some snakes, and this was one of the reasons why the bone was previously identified as the squamosal. The supratemporal of *Utatusaurus*, however, is of moderate size, so this bone seems to have progressively increased in size in the Ichthyosauria.

Most major amniote groups, and even some non-amniote tetrapods, have at some time been proposed to be the sister group of ichthyosaurs<sup>5</sup>. Although a consensus is emerging that ichthyosaurs are diapsids<sup>5,6,10,11,23</sup>, there is still opposition<sup>17,24</sup>, largely because of the lack of information about the basal ichthyosaurs<sup>6,17</sup>. Two recent cladistic studies concluded that the Ichthyosauria is the sister group of the Sauropterygia (which includes plesiosaurs and placodonts), which together form the sister group of the archosauromorphs<sup>10,11</sup>. However, only limited data from basal ichthyosaurs were available for these studies<sup>10,11</sup>, and re-examination of one of the data matrices<sup>10</sup> revealed that about a third of the characters would be coded differently if *Utatusaurus* were included. Moreover, this placement of sauropterygians disagrees with the more widely accepted hypothesis, in which sauropterygians are more closely related to lepidosaurs than to archosaurs<sup>8,9</sup>. To test these competing hypotheses, we reanalysed two data matrices<sup>9,10</sup> by incorporating the data obtained from the new specimens of *Utatusaurus*. In both cases (Fig. 3), ichthyosaurs appeared within the Diapsida but outside the Sauria, whereas sauropterygians were separated from ichthyosaurs and formed a clade with lepidosauromorphs. The new specimens of *Utatusaurus* confirm once again the importance of basal taxa to the assignments of character polarities and to the outcome of phylogenetic analyses<sup>25</sup>. □

**Methods**

**Retrodeformation.** The effects of tectonic deformation on taxonomy are important in invertebrate palaeontology<sup>26,27</sup>. Information available for the retrodeformation of a vertebrate fossil is usually limited, but the original shape can be restored with as few as two pairs of measurements<sup>7</sup>. The dorsal view of the skull, which is not parallel to the bedding plane, was retrodeformed according to the measurements from the skull roof itself, as described<sup>7</sup>. The image of the entire skeleton along the bedding plane was retrodeformed, based on measurements from the vertebral centra made according to ref. 28 and confirmed as described in ref. 7. In both cases, the bilateral symmetry of the body was well restored.

**Phylogenetic analyses.** The first phylogenetic hypothesis (Fig. 3a) was derived by adding the Ichthyosauria to the data matrix of Rieppel and DeBraga<sup>9</sup> (see Supplementary Information). Several character codings were amended according to ref. 29. In addition, the following characters were modified: 30, there is no supratemporal in sauropterygians (recoded); 33, there is no posterior process on the jugal in basal ichthyosaurs (new character state added); 83, the coronoid process is present on the surangular in ichthyosaurs (new character state added). Two characters, namely (162) short limbs and (163) short manus/pes, were omitted because limb, manus and pes each comprise multiple elements, and the whole structure may be shortened in many different ways; and because such shortenings are also known in other aquatic tetrapods with different origins, such as cetaceans and mosasaurs, so they probably reflect aquatic adaptation rather than a common origin. The second phylogenetic hypothesis (Fig. 3b) was derived by recoding ichthyosaurs in the data matrix of Caldwell<sup>10</sup>. Only ichthyosaurian characters were recoded in the modified character matrix (see Supplementary Information). In both cases, the ichthyosaurian characters were coded according to *Utatusaurus*; in the absence of information for *Utatusaurus*, references were made to successively more derived ichthyosaurs, namely *Chensaurus*, *Cymbospondylus* and *Ichthyosaurus*. All phylogenetic analyses were made by using the heuristic search option of PAUP 3.1.1 (100 random addition sequences for both TBR and SPR)<sup>30</sup>.

Received 12 November 1997; accepted 23 February 1998.

1. McGowan, C. *Dinosaurs, Spiffires, and Sea Dragons* (Harvard Univ. Press, Cambridge and London, 1991).
2. Motani, R., You, H. & McGowan, C. Eel-like swimming in the earliest ichthyosaurs. *Nature* **382**, 347–348 (1996).

3. Carroll, R. L. Evolutionary constraints in aquatic diapsid reptiles. *Spec. Pap. Palaentol.* **33**, 145–155 (1985).
4. Carroll, R. L. & Dong, Z. M. *Hupehsuchus*, an enigmatic aquatic reptile from the Triassic of China, and the problem of establishing relationships. *Phil. Trans. R. Soc. Lond. B* **331**, 131–153 (1991).
5. Callaway, J. M. *Systematics, Phylogeny, and Ancestry of Triassic Ichthyosaurs (Reptilia, Ichthyosauria)* (thesis, Univ. Rochester, 1989).
6. Massare, J. A. & Callaway, J. M. The affinities and ecology of Triassic ichthyosaurs. *Geol. Soc. Am. Bull.* **102**, 409–416 (1990).
7. Motani, R. New technique for retrodeforming tectonically deformed fossils, with an example for ichthyosaurian specimens. *Lethaia* **30**, 221–228 (1997).
8. Rieppel, O. Osteology of *Simosaurus gaillardoti* and the relationships of stem-group Sauropterygia. *Fieldiana Geol.* **28**, 1–85 (1994).
9. Rieppel, O. & DeBraga, M. Turtles as diapsid reptiles. *Nature* **384**, 453–454 (1996).
10. Caldwell, M. W. Ichthyosauria: A preliminary phylogenetic analysis of diapsid affinities. *N. Jb. Geol. Paläontol. Abh.* **200**, 361–386 (1996).
11. Merck, J. W. A phylogenetic analysis of the euryapsid reptiles. *J. Vert. Paleontol.* **17** (suppl.), 65A (1997).
12. Minoura, N. et al. Excavation of Early Triassic ichthyosaurian fossils from Ogatsu, Miyagi Pref., Japan. *Geol. Stud.* **42**, 215–232 (1993).
13. Minoura, N. in *Paleoasian Ocean to Paleo-Pacific Ocean* 64–68 (Hokkaido Univ., Sapporo, 1994).
14. Shikama, T., Kamei, T. & Murata, M. Early Triassic Ichthyosaurus, *Utatusaurus hataii* gen. et sp. nov., from the Kitakami Massif, Northeast Japan. *Sci. Rep. Tohoku Univ., Sendai, Second Ser. (Geol.)* **48**, 77–97 (1978).
15. Motani, R. Phylogeny of the Ichthyosauria (Amniota: Reptilia) with special reference to Triassic forms. *J. Vert. Paleontol.* **17** (suppl.), 66A (1997).
16. Romer, A. S. *Osteology of the Reptiles* (Univ. Chicago Press, Chicago and London, 1956).
17. Maisch, M. W. A case against a diapsid origin of the Ichthyosauria. *N. Jb. Geol. Paläontol. Abh.* **205**, 111–127 (1997).
18. Williston, S. W. *Osteology of the Reptiles* (Harvard Univ. Press, Cambridge, MA, 1925).
19. McGowan, C. The cranial morphology of the Lower Liassic latipinnate ichthyosaurs of England. *Bull. Br. Mus. Nat. Hist. Geol.* **24**, 1–109 (1973).
20. Romer, A. S. An ichthyosaur skull from the Cretaceous of Wyoming. *Contrib. Geol. Univ. Wyo.* **7**, 27–41 (1968).
21. Kirton, A. M. *A Review of British Upper Jurassic Ichthyosaurs* Thesis (Univ. Newcastle, 1983).
22. Godefroit, P. The skull of *Stenopterygius longifrons* (Owen, 1881). *Rev. Paléobiol., Genève, Vol. Spéc. 7*, 67–84 (1993).
23. Tarsitano, S. A model for the origin of ichthyosaurs. *N. Jb. Geol. Paläontol. Abh.* **164**, 143–145 (1982).
24. Riess, J. Fortbewegungsweise, Schwimmphysik, und Phylogenie der Ichthyosaurier. *Palaentogr. Abt. A* **192**, 93–155 (1986).
25. Gauthier, J., Kluge, A. G. & Rowe, T. Amniote phylogeny and the importance of fossils. *Cladistics* **4**, 105–209 (1988).
26. Cooper, R. A. Interpretation of tectonically deformed fossils. *N. Z. J. Geol. Geophys.* **33**, 321–332 (1990).
27. Hughes, N. C. & Jell, P. A. A statistical/computer graphic technique for assessing variation in tectonically deformed fossils and its application to Cambrian trilobites from Kashmir. *Lethaia* **25**, 317–330 (1992).
28. Ando, T., Kawamura, M. & Minoura, N. Restoration of tectonically deformed Early Triassic ichthyosaurs. *Abstr. Progr. 1997 Annu. Meet. Geol. Soc. Japan* 160 (1997).
29. Lee, M. Reptile relationships turn turtle. *Nature* **389**, 245–246 (1997).
30. Swofford, D. L. *PAUP 3.1.1* (Smithsonian Inst., Washington DC, 1993).

Supplementary information is available on Nature's World-Wide Web site (<http://www.nature.com>) or as paper copy from Mary Sheehan at the London editorial office of Nature.

**Acknowledgements.** We thank C. McGowan for his support; K. Padian for reading the manuscript; M. Caldwell, A. Hungerbühler, M. Kawamura, J. Merck and H.-D. Sues for discussions; Y. Tomida and M. Manabe for support at NSM; T. Kato, T. Kuwajima, G. Kawakami, H. Normura, D. Suzuki, M. Takahashi for technical support; and the Fujiwara Natural History Foundation, Tokyo, and Miller Institute for Basic Research in Science, Berkeley (R.M.) and the Fukuda Geological Institute (N.M.) for financial support.

Correspondence and requests for materials should be addressed to R.M. (e-mail: [motani@ucmp1.berkeley.edu](mailto:motani@ucmp1.berkeley.edu)).

## Dynamics of North American breeding bird populations

Timothy H. Keitt\* & H. Eugene Stanley†

\* Santa Fe Institute, 1399 Hyde Park Road, Santa Fe, New Mexico 87501, USA and National Center for Ecological Analysis and Synthesis, University of California Santa Barbara, 735 State Street, Suite 300, Santa Barbara, California 93101, USA

† Center for Polymer Studies and Department of Physics, Boston University, Boston 02215, USA

Population biologists have long been interested in the variability of natural populations<sup>1–6</sup>. One approach to dealing with ecological complexity is to reduce the system to one or a few species, for which meaningful equations can be solved. Here we explore an alternative approach<sup>7,8</sup> by studying the statistical properties of a data set containing over 600 species, namely the North American breeding bird survey<sup>9</sup>. The survey has recorded annual species abundances over a 31-year period along more than 3,000 observation routes<sup>10</sup>. We now analyse the dynamics of population

variability using this data set, and find scaling features in common with inanimate systems composed of strongly interacting subunits<sup>11</sup>. Specifically, we find that the distribution of changes in population abundance over a one-year interval is remarkably symmetrical, with long tails extending over six orders of magnitude. The variance of the population over a time series increases as a power-law with increasing time lag, indicating long-range correlation in population size fluctuations<sup>12</sup>. We also find that the distribution of species lifetimes (the time between colonization and local extinction) within local patches is a power-law with an exponential cutoff imposed by the finite length of the time series. Our results provide a quantitative basis for modelling the dynamics of large species assemblages.

For each of the approximately 2,500 routes surveyed in a given year, the North American Breeding Bird Survey (NA BBS) gives  $N_s(t)$ , the number of birds of a given species  $s$  detected on a given route in year  $t$ . The challenge is to extract information relevant to population variability from these data.

We are interested in the dynamics, so we must compare values of  $N_s(t)$  in successive years. We form the quantities  $R_s(t) \equiv N_s(t + 1)/N_s(t)$ , which give the rate of increase or decrease of each species on each route. As population growth is multiplicative, the distribution of abundance  $N_s(t)$  of a species through time is often approximately log-normal<sup>13–15</sup>. The ratio of two numbers, each drawn from a log-normal distribution, is also log-normally distributed, so we might expect that the distribution of  $R_s(t)$  would be log-normal as well. We find that the distribution of  $R_s(t)$  is not log-normal, but is instead power-law, with the tails separated by six orders of magnitude (Fig. 1a), such that

$$P(R_s) \propto \begin{cases} R_s^\alpha & \text{if } R_s \leq 1 \\ R_s^{-\alpha} & \text{if } R_s \geq 1 \end{cases} \quad (1)$$

where the exponent  $\alpha = 2$ . Thus, for the species considered here, there is no characteristic scale of fluctuation in population size, but instead we find a broad spectrum of growth rates.

We may also consider the more commonly used<sup>16,17</sup> logarithm of the ratio of successive abundances,  $r_s \equiv \log R_s$ . Equation (1) then becomes  $P(r_s) \propto \exp(-\alpha|r_s|)$ .

What is remarkable about the results shown in Fig. 1a is that, despite the inclusion of a large number of species, the overall

distribution can be described by relatively simple mathematical equations. The distribution is highly symmetrical, so exactly as many species are increasing in abundance as are decreasing.

In this analysis, the quantities  $R_s(t)$  and  $r_s(t)$  measure fluctuations in population size over a one-year interval. It is also possible to analyse the data set for an arbitrary time lag  $\Delta t$ , where  $\Delta t$  can take any value from 1 to 30. We might expect that the variance of the distribution functions corresponding to Fig. 1a will increase with the magnitude of  $\Delta t$  (refs 18, 19). We do indeed find an increase (Fig. 1b), and moreover this increase is a power law of the form  $(\Delta t)^{2H}$ , where  $H$  is the Hurst exponent. For a random walk, successive changes are uncorrelated. The variance of a random walk increases at a particular rate  $H = 0.5$ . Complex dynamics generate serial correlations over time so that the variance increases more rapidly ( $H > 0.5$ ) or more slowly ( $H < 0.5$ ) than for a random walk. For the NA BBS data, we find  $H = 0.14$ , a value considerably smaller than 0.5, which implies the existence of long-range correlations. Correlation in population fluctuations could also arise from correlations in climate variables that influence reproduction and mortality<sup>20</sup> (for example, the severe North American winter of 1975–1976 is thought to have caused large declines in the numbers of some resident bird species<sup>21–23</sup>).

Fluctuations in population size can lead to local extinctions<sup>24,25</sup> and turnover in local species composition<sup>26</sup>. For example, survivorship of local spider populations on Caribbean islands followed a hollow curve that deviated from exponential<sup>27</sup>. Differences in survivorship among species were attributed to different species-specific life-history strategies. Local extinction dynamics can also be studied quantitatively by considering the distribution of ‘lifetimes’ of species within a local region<sup>28</sup>. We define the lifetime of a species as  $\tau \equiv t_e - t_c$ , where  $t_c$  denotes the year in which the species colonized a patch (the first year that the species was recorded on a given route), and  $t_e$  denotes the year that the species became locally extinct (the last year that the species was recorded on that route). The distribution of species’ lifetimes for the NA BBS data follows a Yule distribution described by a power law, modified by an exponential cutoff (Fig. 2a)

$$P(\tau) = A\tau^{-\alpha}e^{-\tau/\tau_{ch}} \quad (2)$$

where  $\tau_{ch}$  sets the timescale at which the power-law scaling no longer

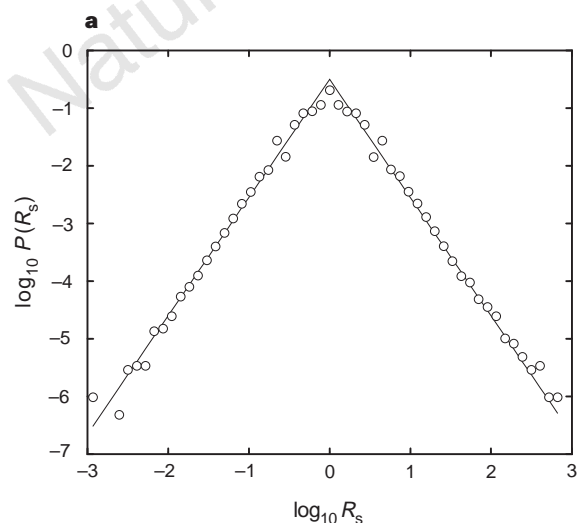
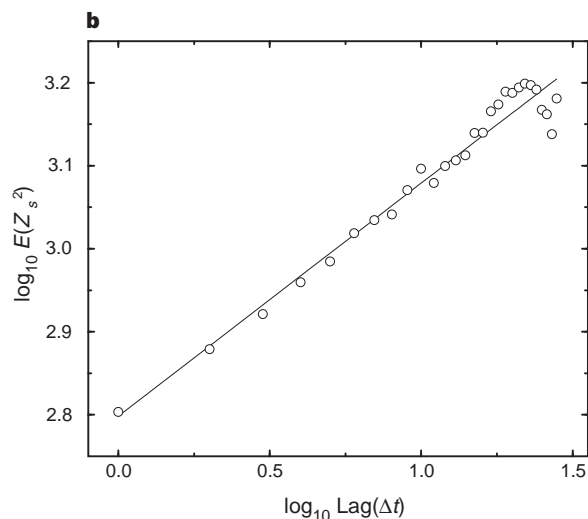


**Figure 1** Scaling of population growth rates in the NA BBS data set. **a**, Distribution of population growth rates  $R_s \equiv N_s(t + 1)/N_s(t)$  across all species in the data. The growth rate  $R_s$  is calculated by dividing species abundances in successive years. Abundances are taken as the total number of individuals of a particular species counted within each survey route. The histogram values at the centre of the distribution are probably influenced by Poisson sample error present in small counts. In a separate analysis, we exclude small counts and find that the tails of



the distribution are unaffected. **b**, Characterization of fractal scaling in population dynamics. The variance of the fluctuation distribution  $E(Z_s^2)$  increases as a power-law function of time lag  $\Delta t$ , where  $Z_s \equiv N_s(t + 1) - N_s(t)$ . Because the number of points separated by a given lag  $\Delta t$  decreases rapidly with increasing lag, deviations from power-law scaling are expected for lags approaching the 31-year length of the time series. The slope of 0.28 corresponds to a Hurst exponent of 0.14.

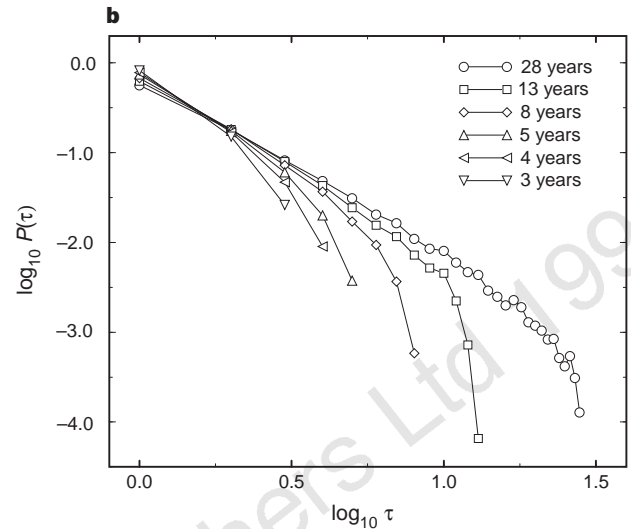
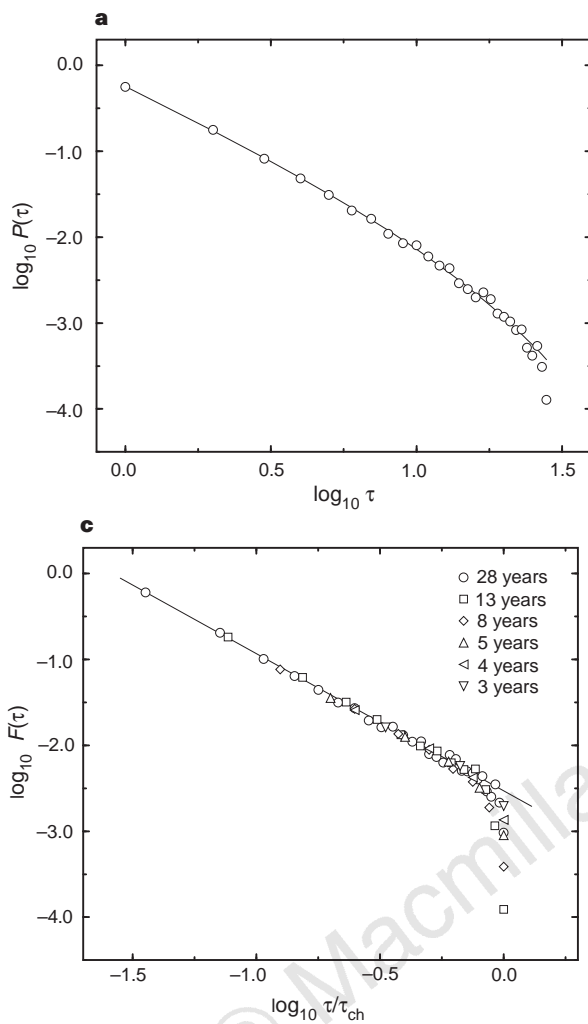


**Figure 2** Scaling of local species' lifetimes in the NA BBS data set. **a**, Frequency distribution of species lifetimes within local patches for all species. Parameters of the data fit are obtained by weighted least-squares regression. The sum of the distribution is normalized to unity. The lifetime of a species within a patch is the time between colonization and local extinction. Colonization occurs when a species is recorded, but was absent the previous year; extinction occurs when a species is absent, but was recorded the previous year. Time series not surveyed in each year between colonization and extinction are not included, as well as time series that begin or end in the first or last year of the survey data. **b**, Finite size analysis of the species' lifetime distribution. The distributions are from non-overlapping subsets of each time series, broken into increasingly shorter sequences. The number of years shown are the maximum possible species' lifetimes between the first and last year of the individual time series. **c**, Test of generality of species' lifetimes distribution. When axes are rescaled to remove finite scaling effects, the data collapse onto a single power-law curve. For each finite subset of the data, we compute  $F(\tau) = P(\tau)/A\tau^{-\alpha}e^{-\tau/\tau_{ch}}$  and plot  $F(\tau)$  against the rescaled time axis  $\tau/\tau_{ch}$ .

holds owing to the finite size of the data set. We find that  $\alpha = 1.61 \pm 0.02$  and  $\tau_{ch} = 14$  years for the NA BBS data. The parameter  $A$  is an arbitrary normalization constant.

The exponential term in equation (2) introduces a characteristic timescale of  $\tau_{ch} = 14$  years into the distribution of extinction times. We can test whether the exponential term is due to finite size effects by plotting a series of lifetime distributions, each computed from non-overlapping subsets of the time series associated with each survey route (Fig. 2b). The resulting distributions are increasingly truncated by the lengths of the time series. When plotted on rescaled axes (Fig. 2c), the distributions collapse onto a single power-law curve. Thus, we find that the power-law distribution is unaffected by shortening the time series; only the exponential term is affected, suggesting that the power-law behaviour extends beyond the 31-year extent of this data set.

The presence of scaling, both in population variability (Fig. 1a) and in local species' lifetimes (Fig. 2c), may have implications for understanding population dynamics in general. Scaling of system variables is often observed in physical systems that exhibit cooperative behaviour<sup>29,30</sup>. Scaling arises in these inanimate systems because each particle interacts directly with a few neighbouring particles and as these neighbouring particles interact with their neighbours, interactions can 'propagate' long distances, resulting in power-law distributions. Similarly, species in an ecosystem interact directly with some (but not all) other species, which in turn interact with other species so that interactions can 'propagate'.

Interactions can propagate not only among species in an ecosystem, but through space as well. In both island biogeography<sup>31</sup> and metapopulation theory<sup>24</sup>, the probability of a patch (island) being

occupied is often modelled by the incidence function  $P(x_i = 1) = c_i/c_i + e_i$ , where  $x_i = 1$  if the patch is occupied,  $c_i$  is the colonization probability, and  $e_i$  is the extinction probability<sup>26,32</sup>. On islands, where distances between populations are large, we expect that the species lifetime distribution should decay exponentially, because the probability  $P(x_i = 1)$  is roughly constant. However, metapopulations are often more strongly coupled than island populations, and can experience a much stronger 'rescue effect'<sup>33</sup> whereby local populations are saved from extinction by immigration from nearby patches. This rescue effect may explain the long-tailed distribution of species lifetimes. □

Received 23 December 1997; accepted 19 February 1998.

1. May, R. M. Biological populations with nonoverlapping generations: Stable points, stable cycles, and chaos. *Science* **186**, 645–647 (1974).
2. Ives, A. R. Chaos in time and space. *Nature* **353**, 214–215 (1991).
3. Turchin, P. Rarity of density dependence or population regulation with lags? *Nature* **344**, 660–663 (1990).
4. Arino, A. & Pimm, S. L. On the nature of population extremes. *Evol. Ecol.* **9**, 429–443 (1995).
5. Rhodes, C. J. & Anderson, R. M. Power laws governing epidemics in isolated populations. *Nature* **381**, 600–602 (1996).
6. Curnutt, J. L., Pimm, S. L. & Maurer, B. A. Population variability of sparrows in space and time. *OIKOS* **76**, 131–144 (1996).
7. Brown, J. H. *Macroecology* (Univ. of Chicago Press, Chicago, 1995).
8. Keitt, T. H. & Marquet, P. A. The introduced Hawaiian avifauna reconsidered: Evidence for self-organized criticality? *J. Theor. Biol.* **182**, 161–167 (1996).
9. Peterjohn, B. G. The North American breeding bird survey. *J. Am. Birding Assoc.* **26**, 386–398 (1994).
10. Sauer, J. R., Hines, J. E., Gough, G., Thomas, I. & Peterjohn, B. G. *The North American breeding bird survey results and analysis, version 96.3* (Patuxent Wildlife Research Center, Laurel, MD, 1997). (<http://www.mbr.nbs.gov/bbs/bbs.html>)
11. Stanley, M. H. R. *et al.* Scaling behaviour in the growth of companies. *Nature* **379**, 804–806 (1996).
12. Beran, J. *Statistics for Long Memory Processes* (Chapman and Hall, New York, 1994).
13. Preston, F. W. The canonical distribution of commonness and rarity: I. *Ecology* **43**, 185–215 (1962).
14. MacArthur, R. H. On the relative abundance of bird species. *Proc. Natl Acad. Sci. USA* **43**, 293–295 (1957).
15. Sugihara, G. Minimal community structure: An explanation of species abundance. *Am. Nat.* **116**, 770–787 (1980).

16. Hassell, M. P., Lawton, J. H. & May, R. M. Patterns of dynamical behavior in single-species populations. *J. Anim. Ecol.* **45**, 471–486 (1976).
17. Royama, T. *Analytical Population Dynamics* (Chapman and Hall, London, 1992).
18. Connell, J. H. & Sousa, W. P. On the evidence needed to judge ecological stability or persistence. *Am. Nat.* **121**, 789–824 (1983).
19. Pimm, S. L. & Redfearn, A. The variability of population densities. *Nature* **334**, 613–614 (1988).
20. Steele, J. H. A comparison of terrestrial and marine ecological systems. *Nature* **313**, 355–358 (1985).
21. Pitts, T. D. Eastern bluebird populations fluctuations in Tennessee during 1970–1979. *The Migrant* **52**, 29–37 (1981).
22. Sauer, J. R. & Droege, S. Recent population trends of the eastern bluebird. *Wilson Bull.* **102**, 239–252 (1990).
23. Sauer, J. R., Pendleton, G. W. & Peterjohn, B. G. Evaluating causes of population change in North American insectivorous songbirds. *Conservation Biol.* **10**, 465–478 (1996).
24. Hanski, I. & Gilpin, M. Metapopulation dynamics: Brief history and conceptual domain. *Biol. J. Linn. Soc.* **42**, 3–16 (1991).
25. Hanski, I., Foley, P. & Hassell, M. Random walks in a metapopulation: How much density dependence is necessary for long-term persistence? *J. Anim. Ecol.* **65**, 274–282 (1996).
26. Diamond, J. M. & May, R. M. Species turnover rates on islands: Dependence on census interval. *Science* **197**, 266–270 (1977).
27. Schoener, T. W. & Spiller, D. A. High population persistence in a system with high turnover. *Nature* **330**, 474–477 (1987).
28. Pimm, S. L., Diamond, J., Reed, T. M., Russell, G. J. & Verner, J. Times to extinction for small populations of large birds. *Proc. Natl. Acad. Sci. USA* **90**, 10871–10875 (1993).
29. Stanley, H. E. *Introduction to Phase Transitions and Critical Phenomena* (Oxford Univ. Press, Oxford, 1971).
30. Stanley, H. E. Power laws and universality. *Nature* **378**, 554 (1995).
31. MacArthur, R. H. & Wilson, E. O. *Island Biogeography* (Princeton Univ. Press, 1967).
32. Hanski, I. A practical model of metapopulation dynamics. *J. Anim. Ecol.* **63**, 151–162 (1994).
33. Brown, J. H. & Kodric-Brown, A. Turnover rates in insular biogeography: effect of immigration on extinction. *Ecol.* **58**, 445–449 (1977).

**Acknowledgements.** This work was partially supported by the Santa Fe Institute, Thaw Foundation and National Science Foundation. We thank B. Peterjohn and the Patuxent Wildlife Research Center, United States Department of the Interior, for providing the NA BBS data in digital form, and L. A. N. Amaral, P. Bak, J. H. Brown, P. A. Marquet, B. Maurer, R. M. May, B. T. Milne, M. Paczuski, B. Peterjohn, S. L. Pimm, R. V. Solé and M. Taper for their comments.

Correspondence and requests for materials should be addressed to T.H.K. (e-mail: keitt@nceas.ucsb.edu).

## Herbicide resistance caused by spontaneous mutation of the cytoskeletal protein tubulin

Richard G. Anthony, Teresa R. Waldin, John A. Ray\*, Simon W. J. Bright\* & Patrick J. Hussey

School of Biological Sciences, Royal Holloway University of London, Egham Hill, Egham, Surrey TW20 0EX, UK

\* Zeneca Agrochemicals, Jeolott's Hill Research Station, Bracknell, Berkshire RG42 6ET, UK

The dinitroaniline herbicides (such as trifluralin and oryzalin) have been developed for the selective control of weeds in arable crops. However, prolonged use of these chemicals has resulted in the selection of resistant biotypes of goosegrass, a major weed. These herbicides bind to the plant tubulin protein but not to mammalian tubulin<sup>1</sup>. Here we show that the major  $\alpha$ -tubulin gene of the resistant biotype has three base changes within the coding sequence. These base changes swap cytosine and thymine, most likely as the result of the spontaneous deamination of methylated cytosine. One of these base changes causes an amino-acid change in the protein: normal threonine at position 239 is changed to isoleucine. This position is close to the site of interaction between tubulin dimers in the microtubule protofilament. We show that the mutated gene is the cause of the herbicide resistance by using it to transform maize and confer resistance to dinitroaniline herbicides. Our results provide a molecular explanation for the resistance of goosegrass to dinitroaniline herbicides, a phenomenon that has arisen, and been selected for, as a result of repeated exposure to this class of herbicide.

The dinitroaniline herbicides disrupt meristem development in the roots and shoots as a result of the net depolymerization of cellular microtubules<sup>2,3</sup>. The repeated use of the dinitroaniline herbicides on the cotton and soybean fields in North America has resulted in the appearance of biotypes of goosegrass, *Eleusine indica* (Fig. 1), that have evolved resistance to the herbicides<sup>4–6</sup>. Dose–

**Table 1 Differential sensitivity of the sensitive and resistant biotypes to dinitroaniline herbicides and to the structurally unrelated pronamide herbicide**

Herbicide	ID <sub>50</sub> (mg l <sup>-1</sup> )		R/S*
	Sensitive	Resistant	
Trifluralin	0.04	1.70	42.5
Oryzalin	0.01	0.60	60.0
Pronamide	0.55	0.59	1.1

The ID<sub>50</sub> value was calculated from seedling dose–response curves.

\* Ratio of ID<sub>50</sub> for resistant biotype to ID<sub>50</sub> for susceptible biotype.

response studies in the laboratory<sup>6</sup> showed that a dinitroaniline-resistant biotype tolerated up to 60-fold higher concentrations of herbicide than did the dinitroaniline-sensitive biotype, but that both biotypes were equally sensitive to the structurally unrelated antimicrotubule herbicide pronamide<sup>7</sup> (Table 1). It is reasonable to propose, in light of the effect of dinitroanilines on plant microtubules<sup>1,8</sup>, that a mutation has arisen in a microtubule protein. In a preliminary investigation we showed that the major  $\alpha$ -tubulin isotype in the resistant biotype had an altered electrophoretic mobility on two-dimensional gels compared to the isotype of the sensitive biotype. In further experiments we focused on a molecular analysis of the  $\alpha$ -tubulin genes.

We constructed two complementary DNA libraries in UniZAP vectors (Stratagene), using poly(A)<sup>+</sup> RNA isolated from seedlings derived from selfed sensitive and resistant biotypes. The sensitive-biotype library was probed with radiolabelled *Zmtua1*, a maize  $\alpha$ -tubulin cDNA clone<sup>9</sup>. We obtained 13 clones that hybridized to the maize  $\alpha$ -tubulin probe. DNA sequencing revealed that 11 of the 13 cDNA clones had identical 3' non-coding regions, indicating that these represented the most prevalent  $\alpha$ -tubulin transcript. This group included the full-length cDNA clone *EiStua1*. The remaining two clones were distinct from the prevalent cDNA and from each

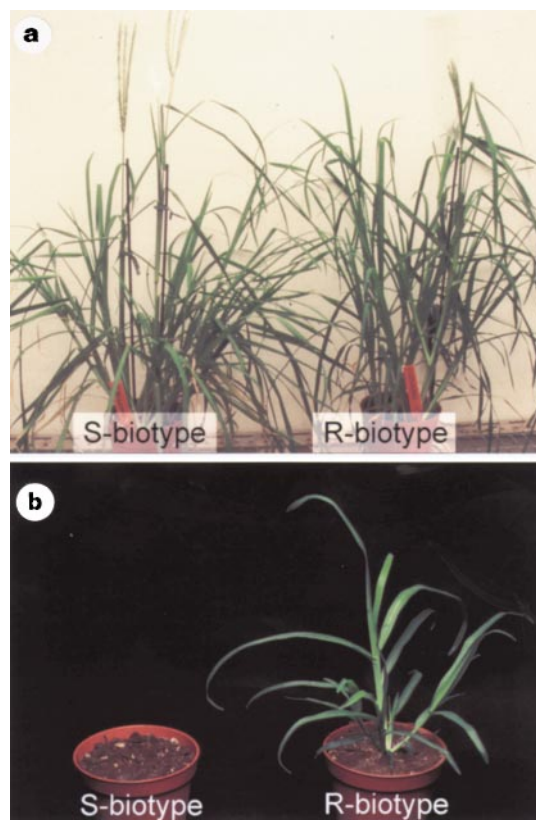


**Figure 1** Dinitroaniline-sensitive (S) and -resistant (R) biotypes of *Eleusine indica* (goosegrass). **a**, S and R biotypes grown to maturity in the absence of herbicide. **b**, S and R biotypes grown on a discriminatory dose of trifluralin (1 mg l<sup>-1</sup>).